

One-Step Synthesis of Zirconia and Magnetite Nanocomposite Immobilized Chitosan for Micro-Solid-Phase Extraction of Organophosphorous Pesticides from Juice and Water Samples Prior to Gas Chromatography/Mass Spectroscopy

Nadereh Rahbar^{1,2} · Elnaz Behrouz¹ · Zahra Ramezani^{1,2}

Received: 21 September 2016 / Accepted: 13 December 2016 / Published online: 10 January 2017
© Springer Science+Business Media New York 2017

Abstract In this research, a magnetic sorbent was prepared by immobilizing zirconia and magnetite (Fe₃O₄) nanoparticles in chitosan, which is characterized and used as an effective nanosorbent in magnetic dispersive micro-solid-phase extraction (MDMSPE) of organophosphorous pesticides (OPPs) from juice and water samples prior to gas chromatography-mass detection (GC-MS). The properties and morphology of synthesized sorbent were characterized by scanning electron microscopy (SEM), Fourier transform-infrared spectroscopy (FT-IR), vibrating sample magnetometry (VSM), and differential scanning calorimetric (DSC) analysis. The main experimental parameters including pH level, extraction time, sorbent mass, salt concentration, and desorption conditions were investigated and optimized to maximize extraction efficiency. Under optimized conditions, the calibration curves were obtained in the concentration range of 0.1–500 ng mL⁻¹ with correlation coefficients between 0.9993 and 0.9999. The limits of detection (signal-to-noise ratio (S/N) = 3) and limits of quantification (S/N = 10) of the method ranged from 0.031 to 0.034 ng mL⁻¹ and 0.105–0.112 ng mL⁻¹, respectively. The intra-day and inter-day RSDs were 2.2–5.7 and 2.5–7.5%, respectively. The method was successfully applied to the analysis of OPPs in fruit juices (apple, peach, and cherry) and

water (mineral, tap, and river) real samples, with recoveries in the range of 86.0–106.0% for the spiked juice and water samples. The results showed that with combination of high selectivity of zirconia and magnetic property of magnetite as well as immobilizing ability of chitosan, the fabricated sorbent exhibited exceptional extraction ability toward the OPPs.

Keywords Zirconia nanoparticles · Magnetite nanoparticles · Organophosphorous pesticides · Magnetic dispersive micro-solid-phase extraction · Gas chromatography · Mass spectroscopy

Introduction

Organophosphorous pesticides (OPPs) as relatively low toxic compounds are used worldwide to increase the yield of agricultural products. However, extensive and incorrect use of them has raised public concern of the potential threat to food and environmental safety. Many international organizations such as the European Union have established maximum residue limits (MRLs) for OPPs in water and food samples in the range of 0.02–0.1 mg L⁻¹ and 0.01–0.5 mg kg⁻¹, respectively (Li et al. 2016; Farajzadeh et al. 2016). Therefore, it is of great importance to develop accurate and sensitive methods for OPP residue analysis in water and food samples.

Generally, sample cleanup and preconcentration of trace analytes from complex matrices like environmental and food samples are required to remove potential interferences prior to instrumental analysis. Solid-phase extraction (SPE) with obvious advantages such as ease of operation, low consumption of toxic solvents, high enrichment factor, flexibility to choose the solid phase, and low cost and time is becoming the most commonly used method for sample preparation in comparison to traditional liquid–liquid extraction (LLE) (Parham et al. 2009;

Electronic supplementary material The online version of this article (doi:10.1007/s12161-016-0769-y) contains supplementary material, which is available to authorized users.

✉ Nadereh Rahbar
n_rahbar2010@ajums.ac.ir; n_rahbar2001@yahoo.com

¹ Nanotechnology Research Center, Faculty of Pharmacy, Ahvaz Jundishapur University of Medical Sciences, Ahvaz, Iran

² Department of Medicinal Chemistry, Faculty of Pharmacy, Ahvaz Jundishapur University of Medical Sciences, Ahvaz, Iran

Wu et al. 2016; Yilmaz and Soylak 2016). However, new miniaturized SPE methodologies (Plotka-Wasyłka et al. 2015) such as dispersive micro-solid-phase extraction (DMSPE) (Asgharinezhad et al. 2014; Wang et al. 2016), micro-solid-phase extraction (MSPE) (Khayoon et al. 2014), solid-phase microextraction (SPME) (Volante et al. 2001; Korba et al. 2013), and stir bar sorptive extraction (SBSE) (Guart et al. 2014) have advantages of suitability for analysis of small amounts of analyte, small sorbent usage, and lower consumption of organic solvents. Based on these miniaturized, sorbent-based extraction methods, a lot of methods have been developed for the analysis of OPPs in real samples such as water, vegetables, and fruit (Galán-Cano et al. 2013; Sang et al. 2013; Wang et al. 2013; Jiang et al. 2016).

Synthesis of novel materials with high selectivity to analytes in order to eliminate the matrix interference and increase sensitivity and accuracy of the extraction method is still an attractive and active research area. It has been reported that zirconia (ZrO_2) nanoparticles (ZNPs) with its high surface area-to-volume ratio, thermal stability, chemical inertness, and lack of toxicity have a strong affinity to phosphoric moieties. They were employed for selective detection of OPPs in electrochemical techniques (Gong et al. 2012; Wang and Li 2008; Mazloum-Ardakani et al. 2010; Parham and Rahbar 2010) and adsorption of phosphate ions (Jiang et al. 2013; Liu et al. 2008; Zong et al. 2013) and phospholipids in removal methods (Lin et al. 2012). Recently, the zirconia-based sorbents have been used in dispersive micro-solid-phase extraction procedures for selective determination of OPPs in water and juice samples (Zare et al. 2016; Jiang et al. 2016). Lewis acid sites on the surface of ZNPs interact strongly with phosphate group as a Lewis base creating coordination bonds (Lozano et al. 2014). However, the small size and possible release into the treated solution restrict their practical applications. Immobilization and encapsulation of nanoparticles with supports such resin, chitosan, and alginate have been effectively used to prevent their leakage into the environment (Kwon et al. 2016).

Chitosan (CS), the deacetylated product of chitin, is a linear polysaccharide (Fig. S1) and has many useful features such as non-toxicity, hydrophilicity, biocompatibility, biodegradability, and antibacterial properties; therefore, it is widely used in food and pharmaceutical processes (Zhou et al. 2010). The applications of CS as a supporting material for the immobilizing of cells and nanoparticles have been previously reported (Namdeo and Bajpai 2008; Jiang et al. 2013; Kwon et al. 2016; Peng et al. 2010).

A major advantage of using magnetite (Fe_3O_4) nanoparticles (MNPs) as the known biocompatible materials is the possibility of particle collection by application of an external magnetic field. Thus, the inclusion of magnetic nanoparticles in one sorbent makes it as an excellent candidate for combining adsorption with ease of phase separation (Parham and Rahbar 2009).

In this work, a new and facile one-step co-precipitation approach was used to fabricate a selective and effective sorbent by immobilization of ZNPs and MNPs with CS in order to prevent their leakage into the environment. Up to our knowledge, this is the first report in application of ZNPs immobilized chitosan for extraction and determination of OPPs with easy separation via MNPs. The synthesized zirconia/magnetite nanocomposite immobilized chitosan (ZMNIC) as a green sorbent was utilized to magnetic dispersive micro-solid-phase extraction (MDMSPE) of methyl parathion (MP), fenitrothion (FT), and malathion (MT) (three most toxic and widely used OPPs) as model analytes from juice and water real samples, coupled with gas chromatography equipped by mass spectrometer detector (GC-MS). Chemical structures of these OPPs are illustrated in Fig. S2.

Experimental

Reagents and Standards

Analytical standards of MP (99.8%), FT (95.8%), and MT (97.3%) were supplied by Fluka. Stock solutions of these compounds were prepared in methanol at a concentration of 500 mg L^{-1} and were stored at -20°C . ZNPs were purchased from Inframat Advanced Materials (Farmington, CT, USA). CS (600–1200 cp and 96% degree of deacetylation) was supplied from Primex (Iceland). $\text{FeCl}_2 \cdot 4\text{H}_2\text{O}$, $\text{FeCl}_3 \cdot 6\text{H}_2\text{O}$, ammonia solution (25%), methanol (MeOH), toluene, *n*-propanol, dichloromethane (DCM), acetone, acetic acid (HOAC), hydrochloric acid (HCl), ammonium hydroxide (25%), sodium hydroxide (NaOH), and sodium chloride (NaCl) were purchased from Merck (Darmstadt, Germany).

Apparatus

Fourier transform-infrared spectroscopy (FT-IR) spectra were recorded by a vertex 70 FTIR spectrometer, in the scanning range of $400\text{--}4000 \text{ cm}^{-1}$ (Bruker, Germany). Differential scanning calorimetric (DSC) analysis was performed using a DSC1 STAR system (Mettler Toledo, Switzerland). Ten milligrams of sample was put in an aluminum pan and heated from 0 to 400°C at a constant heating rate of $10^\circ\text{C}/\text{min}$ under constant purging of nitrogen at 20 mL min^{-1} . Scanning electron microscopy (SEM) and energy-dispersive X-ray diffraction (EDX) were used to show the morphology, dimension, and composition of the ZMNIC (TESCAN, VEGA (II) LMH, Czech Republic). A MDK-VSM system (Meghnatis Daghigh Daneshpajouh Co., Iran) was used to record magnetic properties of the synthesized MNPs and ZMNIC. GC analysis was carried out on an Agilent 7890A instrument (Palo Alto, CA, USA) with split/splitless injection port, and an Agilent 5975C mass detector system was used. The MS detector was operated

in electron impact (EI) mode with ionization energy of 70 eV. Helium (99.999%) was used as the carrier gas at a flow rate of 1 mL min⁻¹. OPPs were separated on a 30 m × 0.320 μm HP-5 MS column with 0.25-μm film thickness. The GC column temperature was first 70 °C (without holding at this temperature), then increased to 150 °C by 25 °C min⁻¹, next raised to 180 °C by increments of 3 °C min⁻¹, and finally increased to 200 °C by increments of 1.5 °C min⁻¹. The split/splitless injection port was set at 250 °C and in splitless mode. The GC-MS interface, ion source, and quadrupole temperatures were set at 280, 230, and 150 °C, respectively. The solvent delay and total run time for analysis were 7 and 22 min, respectively. For quantitative determination, the MS detector was operated in the time-scheduled selected ion monitoring (SIM) mode. The *m/z* values of the selected quantitative ions were 263, 277, and 125 for MP, FT, and MT, respectively. Data acquisition was conducted using ChemStation software. All sample solutions were stirred using a Heidolph magnetic stirrer (Germany). Solvent desorption of OPPs was performed by an ultrasonic bath (Elma, Germany). Solution pH values were measured by a pH meter E520 (Metrohm Herisau, Switzerland). A super magnet (1.2 T, 10 × 5 × 2 cm) was also used.

Synthesis of ZMNIC

A schematic illustration of the synthesis steps for ZMNIC and its proposed structure is demonstrated in Fig. 1a. The sorbent was synthesized by simple a one-step procedure. Briefly, first, 0.1 g of ZNPs in 4 mL of FeCl₃ solution (1/2 mol L⁻¹ HCl solution) was vigorously stirred for 10 min to obtain a homogeneous suspension. Then, 1 mL of FeCl₂ solution (2/2 mol L⁻¹ HCl solution) was added into the prepared suspension, and 50 mL of 1 mol L⁻¹ ammonium hydroxide solution was added dropwise while stirring vigorously. Meanwhile, the 10 mL of CS solution (1% w/v in 5% HAOC aqueous solution) was slowly dripped into the mixture. The obtained suspension was again stirred for 10 min, and the prepared ZMNIC was collected using an external magnetic field and thoroughly washed with deionized water to remove excess ammonium hydroxide. The synthesized sorbent was dried under nitrogen atmosphere and stored in a desiccator before use. The photographs of the sorbent fabrication are presented in the supplementary data (Fig. S3)

Extraction and Analysis

The extraction process was performed in a batch mode. A 5 mL solution containing 0.1–500 ng mL⁻¹ of OPPs and 0.25 mL acetate buffer (pH 5.0) was stirred with 5 mg of dried ZMNIC for 5 min in a glass tube at room temperature. Afterwards, the sorbent was easily separated from the solution using an external magnetic field and washed with deionized water to remove any possible interference. The OPPs were

desorbed from ZMNIC with 2 mL DCM in 7 min using an ultrasonic bath. The solvent of desorption solution was separated from the sorbent with the aid of a magnet and evaporated to dryness under nitrogen gas, and the residue was re-dissolved in 100 μL toluene. Finally, a 1 μL aliquot of obtained solution was injected into the GC-MS (Fig. 1b). Photographs of the system setup are presented in the supplementary data (Fig. S4).

Analysis of Real Samples

A river water sample was collected from the Karun River in Ahvaz (Khuzestan province, Iran). A tap water sample was collected from Ahvaz. Mineral water and juice samples were purchased from local supermarkets in Ahvaz. All samples were filtered through a 0.45-mm membrane filter and stored at 4 °C. Each 5 mL of solution including 2.5 mL of real sample, spiked standard analytes, and 0.25 mL of acetate buffer (pH 5.0) was subjected to the optimized extraction and analytical method without any pretreatments. Extractions from non-spiked samples were also carried out in parallel. All experiments were performed in triplicate. Recovery (*R*%) was calculated using the following equation:

$$R\% = (C_F/C_A) \times 100$$

C_F is the founded concentration in the real samples spiked with a known amount of OPP standard solution, and *C_A* is the added concentration of OPPs in real samples, respectively.

Results and Discussion

Characterization of ZMNIC

Surface area of a sorbent directly affects its extraction efficiency due to enhanced available sites for the adsorption. The morphology and size of the prepared MNPs and ZMNIC were characterized by SEM (Fig. 2). As shown in Fig. 2a, the synthesized MNPs are nano-sized and spherical with a high surface area. Furthermore, ZMNIC particles have small sizes in the range of about 30–45 nm (Fig. 2b), and their morphology is closely similar to that of MNPs, might be due to thin coating of nanoparticles with CS. The results obtained from EDX spectrum confirmed the existence of Fe, Zr, O, and C elements that could be attributed to the presence of MNPs, ZNPs, and CS in ZMNIC (Fig. 2c).

The FT-IR spectra of MNPs, ZNPs, CS, and ZMNIC are illustrated in Fig. 3. As seen in Fig. 3a, the main band at about 508 cm⁻¹ is ascribed to the Zr–O vibration absorption of ZrO₂. The other bands around 1631 and 3430 cm⁻¹ are attributed to the bending and stretching vibration of –OH from adsorbed water molecules. The absorption bands at 570–640 cm⁻¹ are

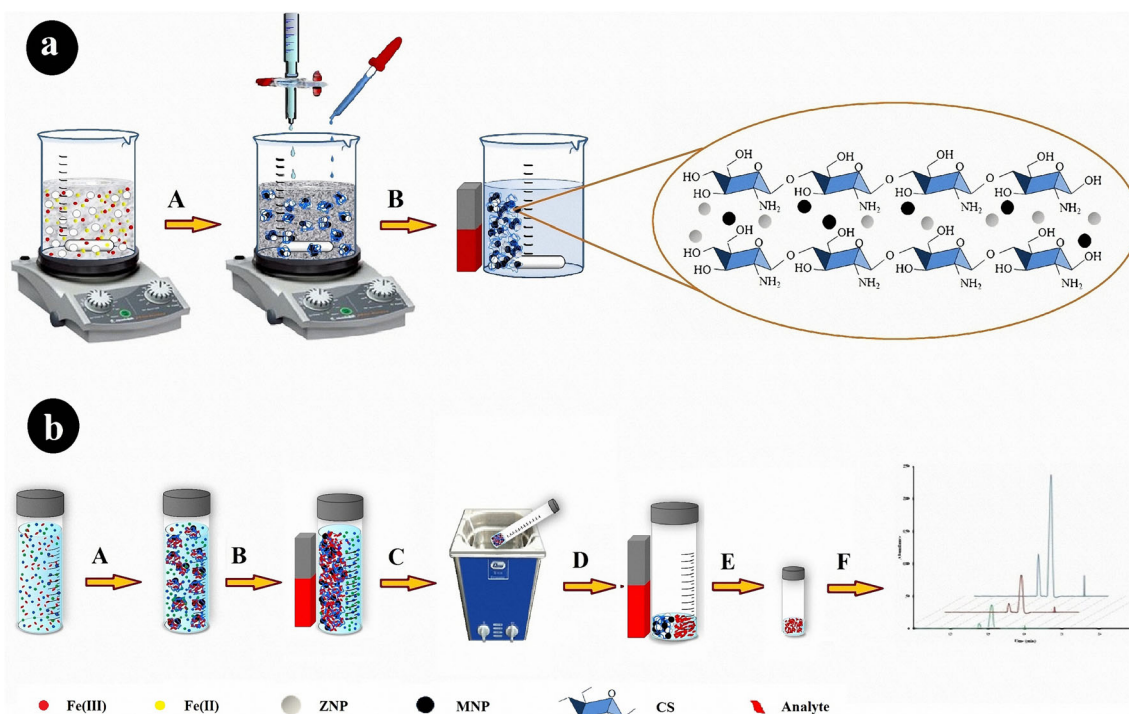


Fig. 1 A schematic illustration of **a** adsorbent synthesis steps: dropwise addition of ammonium hydroxide and CS solutions into homogeneous suspension of ZNPs and Fe(III) and Fe(II) solutions (A) and magnetic separation of the synthesized adsorbent (B); **b** the MDMSPPE procedure: addition of the adsorbent into sample solution and stirring (A), magnetic

separation of the adsorbent from solution (B), desorption under sonication after addition of eluting solvent (C), magnetic separation of eluting solvent (D), transferring of eluting solvent into another tube, evaporation under nitrogen, and adding second solvent (E), and injection to GC-MS (F)

usually attributed to the Fe–O stretches (Parham et al. 2012; Bagheri et al. 2016a,b). In MNP spectrum, the main band at about 591 cm^{-1} and the broad band at around 3439 cm^{-1} are related to the stretching vibrations of Fe–O and –OH from adsorbed water molecules, respectively (Fig. 3b). As shown in Fig. 3c, FT-IR spectrum of CS shows that the presence of intense peaks at 1633 and 1450 cm^{-1} corresponds to –NH bending vibration and deformation vibration in –NH₂ in CS molecules, respectively (Jiang et al. 2013). The other bands at 3426 and 2925 cm^{-1} are related to –OH and –NH, and –CH stretching vibrations, respectively. The absorption peak at 1114 cm^{-1} may be ascribed to the stretching vibration of the

C–O (Jiang et al. 2013; Naing et al. 2016; Jana et al. 2015). The FT-IR spectrum of ZMNIC (Fig. 3d) presents almost all characteristic peaks of the constituents of synthesized sorbent indicating that the sorbent is successfully prepared. Moreover, the characteristic peaks in the CS spectrum (1633 , 1450 , and 1114 cm^{-1}) are shifted to the lower wave numbers (1624 , 1437 , and 1064 cm^{-1}) in the case of ZMNIC, indicating the existence of possible chemical interactions between ZNPs and MNPs with CS. The interaction between Zr(IV) (Lewis acid) and nitrogen of amine group (Lewis base) (appearing bands between 1450 and 1350 cm^{-1}) has been reported in previous studies (Chaufer et al. 2000). As shown in Fig. 3d, the

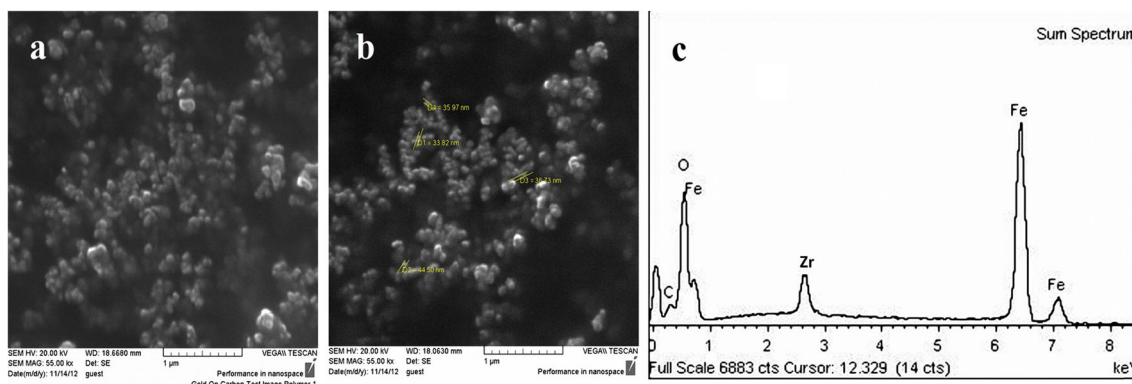
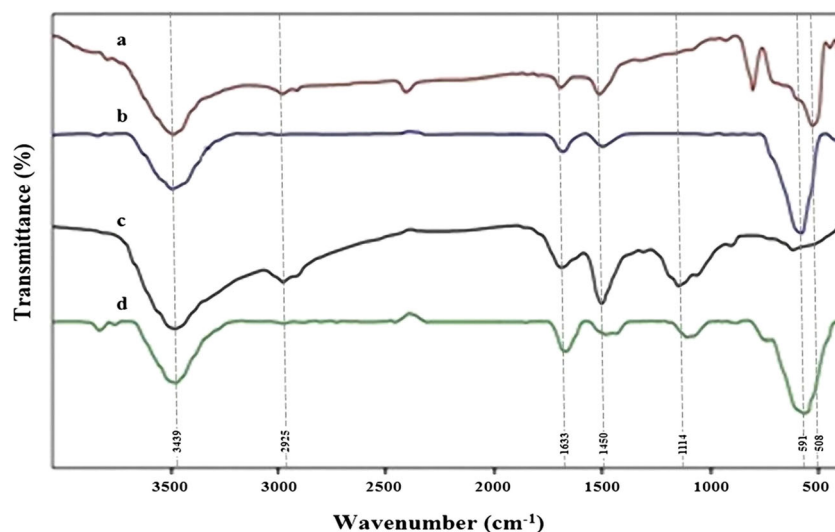


Fig. 2 The morphology and composition: **a** and **b** FESEM images of MNPs and ZMNIC. **c** The EDX spectra of the adsorbent

Fig. 3 FT-IR spectra of ZNPs (a), MNPs (b), CS (c) and ZMNIC (d)



presence of the bands at 1437 and 1385 cm^{-1} can be attributed to such interactions. Similarly, such chemical binding can be suggested between Fe(III) as a Lewis acid and amine and hydroxyl groups in CS. On the other hand, the decreasing intensity at 1437 and 1385 cm^{-1} in the spectrum of ZMNIC (Fig. 3d) compared to 1450 cm^{-1} in CS (Fig. 3c) (related to amide II stretching vibration) indicates that sorbent has lesser active amine groups than CS, probably because of binding with ZNPs and MNPs. Furthermore, the broad and intensive band at 582 cm^{-1} in ZMNIC spectrum is the result of Zr–O and Fe–O overlapping bands.

The magnetic properties of MNPs and ZMNIC were studied by a vibrating sample magnetometer (VSM). As seen in Fig. 4, there are no magnetic hysteresis loops in both curves, revealing super paramagnetic property of the as-prepared magnetic materials (Peng et al. 2015). Moreover, the

saturation magnetization of ZMNIC (44.9 emu g^{-1}) was obviously lower than that of MNPs (68.7 emu g^{-1}), indicating the existence of ZNPs as well as coating of MNPs/ZNP nanocomposite with CS. However, ZMNIC could be rapidly and efficiently separated from sample solution by a magnet because of its relatively high saturation magnetization values.

To examine the thermal properties of MNPs, ZNPs, CS, and ZMNIC materials, their DSC analysis has been carried out as illustrated in Fig. 5. For pure ZrO_2 , the DSC curve shows a broad endothermic peak below 180 $^{\circ}\text{C}$ due to water elimination (Fig. 5a) (Sohn et al. 2001). As shown in Fig. 5b, DSC curve of MNPs exhibits an endothermic peak at nearly 140 $^{\circ}\text{C}$ and a relatively large exothermic effect at about 360 $^{\circ}\text{C}$, which accords with earlier reported studies (Machala et al. 2007). These peaks might be related to the water elimination and crystallization of MNPs, respectively.

Fig. 4 VSM magnetization curves of MNPs (a) and ZMNIC (b)

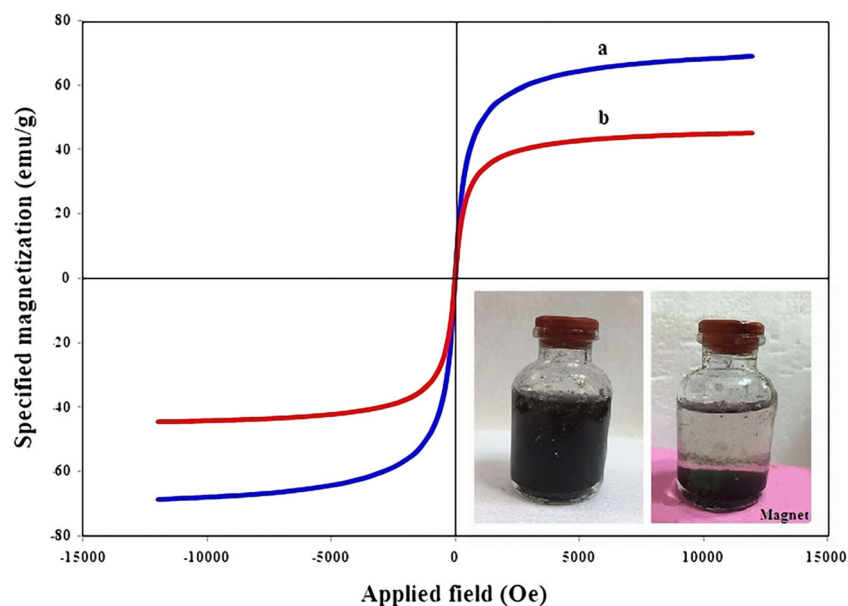
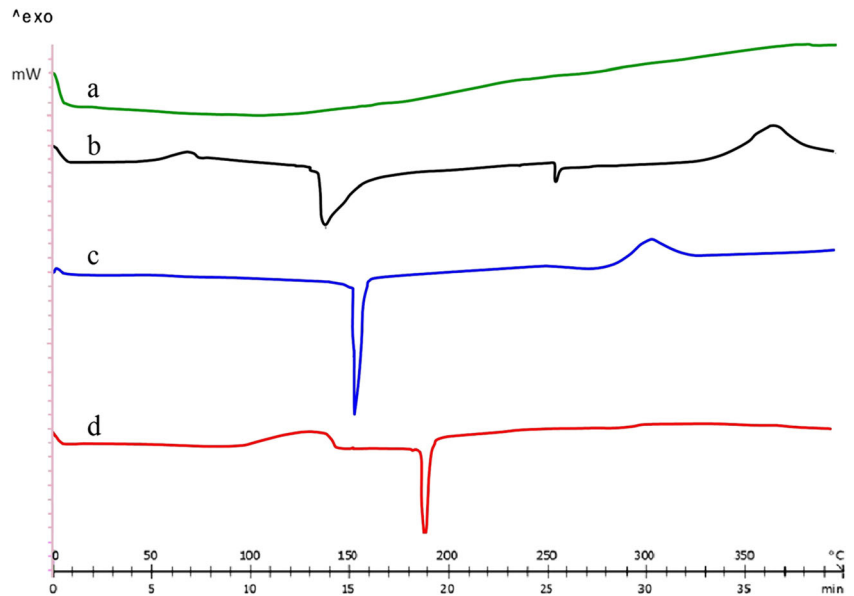


Fig. 5 The DSC curves of ZNPs (a), MNPs (b), CS (c), and ZMNIC (d)



DSC curve of CS presents an endothermic peak at about 150 °C and a broad exothermic peak at nearly 300 °C, which can be correlated to the crystallization of the biopolymer in a different form and decomposition of amine units of the pure CS (Fig. 5c) (Jana et al. 2015). The data presented in Fig. 5d clearly show that the peak corresponding to the decomposition of amine units of pure CS disappeared suggesting that amine groups in ZMNIC have become more stable compared to CS. Moreover, the endothermic peak at about 150 °C in the case of CS and MNPs appeared in the thermogram of ZMNIC at higher temperature. These observations might be attributed

to enhanced sorbent stiffness due to the bonded ZNPs and MNPs to amine groups in ZMNIC and clearly indicates that the nanoparticles could affect the physicochemical characters of the sorbent.

Optimization of Experimental Conditions for MMSPE Procedure

In order to obtain the best extraction efficiency in MMSPE procedure using ZMNIC, influential parameters such as pH, extraction time, sorbent mass, type of desorbing solvent, and

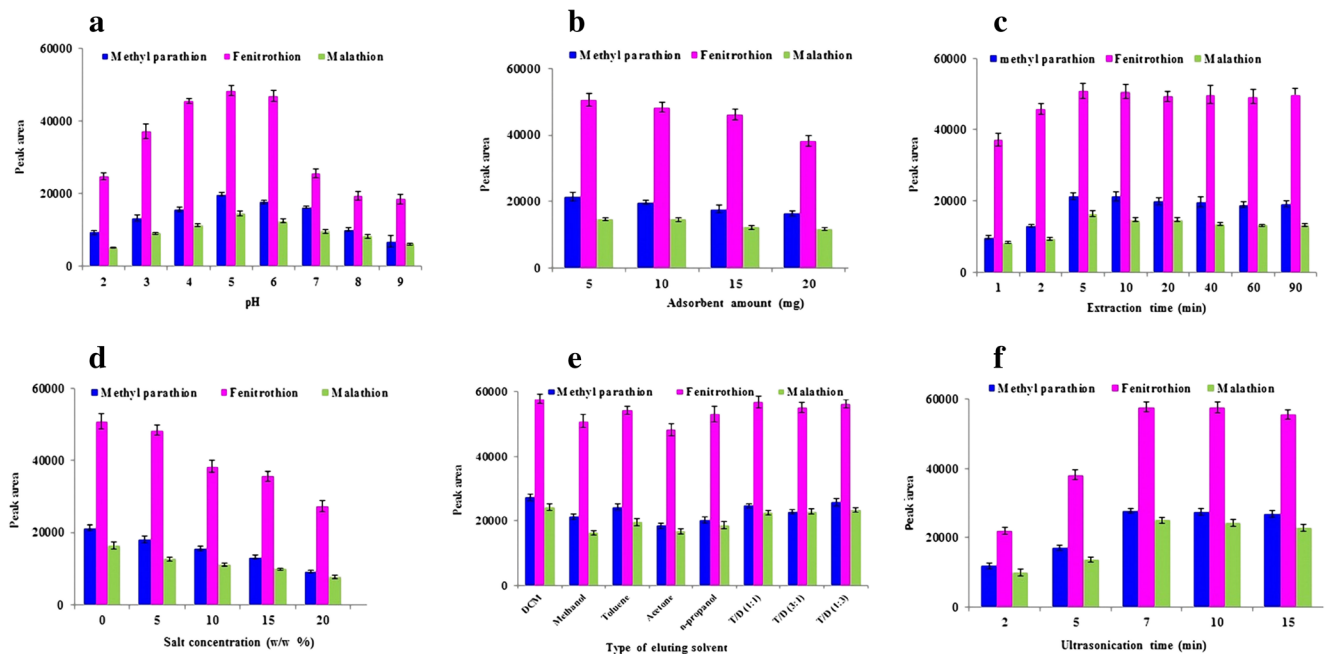


Fig. 6 Effects of various parameters on extraction efficiency: **a** pH, **b** the amount of ZMNIC, **c** extraction time, **d** salt concentration on the extraction efficiency, **e** type of eluting solvent, and **f** sonication time in desorbing step

Table 1 Analytical features for determination of OPPs by the proposed MDMSPE/GC-MS method

Pesticide	LOD	LOQ	LDR	r^a	Regression equation
Methyl parathion	0.034	0.112	0.1–500	0.9998	$y = 561.59x + 130.84$
Fenitrothion	0.031	0.105	0.1–500	0.9993	$y = 1233.2x + 110.62$
Malathion	0.034	0.110	0.1–500	0.9999	$y = 518.41x + 132.2$

LOD limit of detection (ng mL^{-1}), LOQ limit of quantification (ng mL^{-1}), LDR linear dynamic range (ng mL^{-1})

^a Correlation coefficient

its volume along with the sonication time in the desorption step were optimized.

Influence of pH

The pH of the sample solution is a key factor influencing both the characteristics of the sorbent and analytes. To test the effect of pH on the extraction efficiency, experiments were performed within the 3–9 range, in the following conditions: 5 mL of OPP solution, 50 ng mL^{-1} ; extraction time, 10 min; sorbent amount, 5 mg; eluting solvent, 0.5 mL of methanol; sonication time for desorption of analytes, 10 min. The effect of pH on the adsorption and extraction of OPPs with ZMNIC is presented in Fig. 6a. As seen, the pH of the sample solution affects extraction efficiency, and the best value is achieved at pH 5.0. Zirconia acts as a Lewis acid, and the adsorption of OPPs on the ZMNIC surface can be described by the interaction between vacant 3d orbital of Zr(IV) and free electron pairs of phosphate moiety in the OPP neutral molecules, when the surface of the sorbent has neutral charge (Lozano et al. 2014). However, since zirconia is an amphoteric metal oxide (with an isoelectric point of 5.7), its surface behaves like a brönsted acid or base

(Lozano et al. 2014; Jiang et al. 2013; Lin et al. 2012; Shi et al. 2004). Therefore, in pH values lower and higher than the isoelectric point of zirconia, the Lewis acid–base attraction between ZNPs and OPPs weakens, and extraction efficiency decreases because of the presence of H^+ and OH^- ions on the surface of the immobilized ZNPs in ZMNIC. In addition, the isoelectric point Cs is at pH 6.4, which means that existing amine groups in its structure are protonated in pH values lower than 6.4, and in pHs higher than that, these groups are in neutral form (Jiang et al. 2013). Taken together, in pH values lower than 5, Lewis acid–base interaction between ZNPs and OPPs weakens; meanwhile, the repulsion forces between amine group and OPPs decrease, and the analytes adsorb on ZMNIC to some extent via electrostatic attractions. However, when pH values are higher than 5 (higher than CS and ZNP isoelectric points), the extraction efficiencies decrease due to the existence of repulsion forces between basic amine groups on CS and OH^- groups covered ZNPs and OPPs. In addition, the adsorption of OPPs on ZMNIC can be decreased due to their hydrolysis in more acidic and alkaline solutions (Maddah and Shamsi 2012; Liu et al. 2013; Mahpishaniana et al. 2015). Thus, in the remaining experiments, the pH of the sample solutions was

Table 2 Relative recoveries and RSDs of OPP QC samples on three concentration levels

Pesticide	Added ^a	Found ^b	Recovery ^c	RSD	
				Intra-day ($n = 5$)	Inter-day ($n = 3$)
Methyl parathion	5.0	4.8 ± 0.3	96.0	5.7	7.5
	25.0	23.2 ± 0.9	92.8	3.9	5.5
	100.0	98.2 ± 2.7	98.2	2.8	3.7
Fenitrothion	5.0	4.7 ± 0.3	94.0	5.6	6.3
	25.0	26.1 ± 1.0	104.4	4.0	4.5
	100.0	93.7 ± 2.1	93.7	2.2	2.5
Malathion	5.0	4.6 ± 0.3	92.0	5.4	7.2
	25.0	22.9 ± 1.0	91.6	4.2	6.1
	100.0	106.2 ± 2.9	106.2	2.7	3.6

RSD relative standard deviations (%)

^a Spiked concentrations of MP, FT, and MT (ng mL^{-1})

^b Recovered concentrations of MP, FT, and MT (ng mL^{-1}); $x \pm s$ ($n = 5$)

^c Relative recovery (%)

adjusted to 5.0 using 0.25 mL of acetate buffer. The buffer volume effect on extraction efficiency is illustrated in Fig. S5.

Effect of ZMNIC Mass

To achieve the acceptable extraction efficiency, the effect of the ZMNIC amount was investigated in the range of 5–20 mg. The experimental conditions were as follows: 5 mL of OPP solution, 50 ng mL⁻¹; pH, 5.0; extraction time, 10 min; eluting solvent, 0.5 mL of methanol; sonication time for desorption of analytes, 10 min. According to the results, the extraction efficiency was enhanced from 5 to 10 mg of ZMNIC used and remained almost constant in higher weights of sorbent. Therefore, 5 mg of suspension was selected for further experiments (Fig. 6b).

Effect of Extraction Time

To achieve the equilibrium state in MDMSPE procedure, sufficient contact time between analytes and sorbent is required, and therefore, the highest adsorption efficiency is obtained. The extraction times in the range of 1–90 min on a magnetic stirrer at 500 rpm were examined in order to obtain the optimum value. The extraction conditions were as follows: 5 mL of OPP solution, 50 ng mL⁻¹; pH, 5.0; sorbent amount, 5 mg; eluting solvent, 0.5 mL of methanol; sonication time for desorption of analytes, 10 min. As it is illustrated in Fig. 6c, the peak areas increased slightly up to 5 min, and no improvement on the extraction efficiency was observed at higher extraction times; therefore, the extraction time of 5 min was chosen for further experiments. These results indicated that the adsorption kinetics was very fast, and the adsorption process reached equilibrium in a short time.

Influence of Salt Concentration

The existence of salt in the solution can increase the extraction efficiency of the analytes due to the “salting out effect.” However, in some cases, salt addition may reduce the amounts of extracted analytes (Asgharinezhad et al. 2014; Bagheri et al. 2016a,b; Mahpishaniana et al. 2015). Therefore, different amounts of NaCl ranging 0–20% (*w/v*) were added into the sample solutions to check the effect of salt concentration. The extraction conditions were as follows: 5 mL of OPP solution, 50 ng mL⁻¹; pH, 5.0; sorbent amount, 5 mg; extraction time, 5 min; eluting solvent, 0.5 mL of methanol; sonication time for desorption of analytes, 10 min. The results are shown in Fig. 6d indicating that addition of salt reduced the amount of extracted OPPs, might be because of increase in solution viscosity and decrease in mass transfer of analytes from solution to the sorbent (Asgharinezhad et al. 2014; Bagheri et al. 2016a,b). Considering these results and the simplicity of the

extraction procedure, further experiments were performed without adding salt.

Desorption Conditions

The adsorbed analytes should be eluted from the sorbent after extraction by the proper solvent prior to GC/MS analysis. The proper selection of eluting solvent can lead to a better desorption of analytes from the sorbent resulting in higher extraction efficiency. Therefore, desorption of OPPs was performed using different solvents, i.e., methanol, toluene, DCM, acetone, and *n*-propanol, since they are GC/MS compatible solvents. The extraction conditions were as follows: 5 mL of OPP solution, 50 ng mL⁻¹; pH, 5.0; sorbent amount, 5 mg; extraction time, 5 min; volume of eluting solvent, 0.5 mL; sonication time for desorption of analytes, 10 min. As it can be seen in Fig. 6e, the desorption ability of DCM was better than that of other solvents. After that, the influence of selected solvent volume on the extraction efficiency of the examined OPPs was studied. It was found that the analytes could be effectively desorbed by 2 mL of DCM (Fig. S6). In order to achieve the best sonication time in desorbing, different times in the range of 2–10 min were investigated. The best sonication time was found to be 7 min as shown in Fig. 6f.

Analytical Features of the Method

The analytical features of the method (dynamic range of the calibration curve, limit of detection (LOD), limit of quantification (LOQ), accuracy, and precision) are summarized in Tables 1 and 2. To evaluate the developed method under optimal extraction conditions, a series of standard solutions containing MP, FT, and MT in the range of 0.1–500 ng mL⁻¹ at ten selected concentration levels was prepared and analyzed. In all calibration curves, peak areas versus concentrations of analytes were plotted using least squares linear regression method. The external calibration curves with wide linear ranges and satisfactory correlation coefficients (*r*) greater than 0.9993 were observed for all OPPs. Also, the calibration curves were obtained in juice and water samples. Slopes of the calibration curves in water and juice samples were nearly the same as the external calibration curve slopes, and therefore, no matrix-matched calibration plots were required. The LODs and LOQs of the method for the analyzed OPPs were defined as a signal-to-noise (S/N) ratio of 3 and 10, respectively. To obtain the intra-day and inter-day precisions of the proposed method which show the precision and accuracy terms, five similar experiments were carried out for the quality control (QC) samples at concentration levels of 5, 25, and 100 ng mL⁻¹ on the same day and on three consecutive days. The obtained peak areas for the QC samples of OPPs were interpolated from their calibration curves on the same day to give concentrations of the analytes. The resulted RSDs were

Table 3 Application of ZMNIC-based MDMSPE method to real samples

Sample	Added ^a	MP		FT		MT	
		Found ^b	Recovery ^c	Found	Recovery	Found	Recovery
Apple juice	–	ND	–	ND	–	ND	–
	5.0	4.6 ± 0.33	92.0	4.5 ± 0.27	90.0	4.6 ± 0.30	92.0
	25.0	22.8 ± 1.10	91.2	22.9 ± 0.95	91.6	23.5 ± 0.81	94.0
Peach juice	–	ND	–	ND	–	ND	–
	5.0	4.5 ± 0.35	90.0	4.6 ± 0.25	92.0	4.6 ± 0.29	92.0
	25.0	23.3 ± 0.95	93.2	23.3 ± 1.08	93.2	23.2 ± 0.93	92.8
Cherry juice	–	ND	–	ND	–	ND	–
	5.0	4.4 ± 0.31	88.0	4.7 ± 0.25	94.0	4.3 ± 0.29	86.0
	25.0	22.8 ± 1.30	91.2	22.3 ± 0.95	89.2	22.8 ± 0.89	91.2
Mineral water	–	ND	–	ND	–	ND	–
	5.0	5.2 ± 0.24	104.0	4.9 ± 0.34	98.0	5.2 ± 0.35	104.0
	25.0	24.6 ± 0.97	98.4	25.7 ± 1.05	102.8	24.6 ± 0.84	98.4
Tap water	–	ND	–	ND	–	ND	–
	5.0	4.8 ± 0.3	96.0	5.0 ± 0.36	100.0	4.9 ± 0.28	98.0
	25.0	24.3 ± 0.86	97.2	24.7 ± 0.93	98.8	24.0 ± 0.99	96.0
River water	–	ND	–	ND	–	ND	–
	5.0	5.25 ± 0.26	105.0	5.3 ± 0.33	106.0	5.1 ± 0.37	102.0
	25.0	25.8 ± 0.91	103.2	25.7 ± 1.21	102.8	24.6 ± 1.17	98.4

All samples were diluted with deionized water at a ratio of 1:2

ND not detected

^a Spiked concentrations of MP, FT, and MT (ng mL⁻¹)

^b Recovered concentrations of MP, FT, and MT (ng mL⁻¹); $x \pm s$ ($n = 3$)

^c Relative recovery (%)

in the range of 2.2–5.7% for analysis of intra-day spiked samples, revealing the high reproducibility of the proposed method. Moreover, the inter-day precision results were in acceptable range between 2.5 and 7.5%.

Application of the Method to Real Samples

The performance of the optimized analytical procedure was assessed by analyzing different real samples including four

types of fruit juice (apple, peach, and cherry) and three types of water (mineral, tap, and river). The results are shown in Table 3. The extraction recoveries from juice and water real sample solutions containing low, middle, and high concentrations of MP, FT, and MT (5 and 25 ng mL⁻¹) were in the range of 86.0–106.0%. All investigated real samples met the criteria for matrix effect (70–120%) according to the guidance document on analytical quality control and validation procedures for pesticide residue analysis in food and feed (Mahpishanian

Fig. 7 MDMSPE-GC-MS chromatograms for apple juice sample before (a) and after (b) being spiked with OPP standard solutions at 25 and c 100 ng mL⁻¹ concentrations

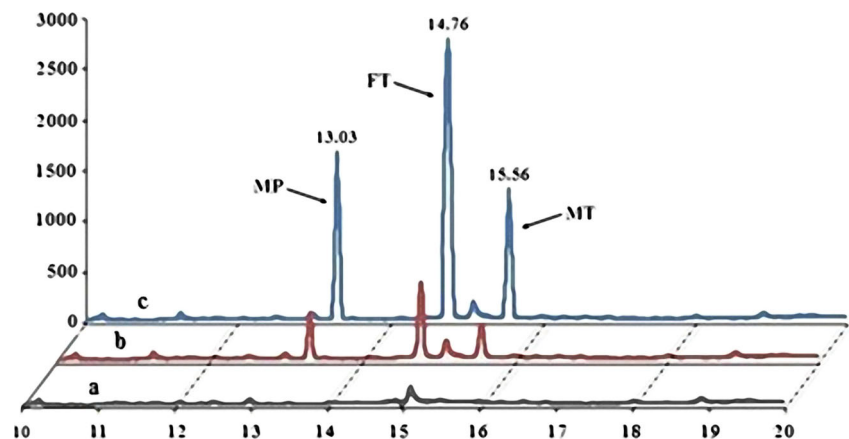


Table 4 Comparison of the current method with other magnetic-based SPE methods for the determination of OPPs

Method	Matrices	LDR (ng mL ⁻¹)	LODs (ng mL ⁻¹)	Extraction time (min)	Recovery (%)	Adsorbent (mg)	References
MSPE-GC-MS	Fruit juice	0.003–50	0.001–0.005	2	86.6–107.5	10	Mahpishanian and Sereshti (2016)
MSPE-GC-MS	Water	100–20,000	0.1–10.30	30	86.9–112.6	1	Jiang et al. (2016)
Magnetic SPE-HPLC-UV	Water	0.05–400	0.0043–0.0474	10	79.6–103.5	20	Heidari and Razmi (2012)
Magnetic SPE-HPLC-UV	Water	100–15,000	26.1–30.2	20	88.5–96.7	100	Li et al. (2013)
MSPE-GC-MS	Water	10–3000	1.8–5.0	10	–	10	Xie et al. (2013)
MDMSPE-GC-MS	Fruit juice-water	0.1–500	0.031–0.034	5	86.0–106.0	5	Present work

and Sereshti 2016). No significant matrix effect for MDMSPE of the selected OPPs by ZMNIC was observed in real samples, indicating that a good selectivity was obtained using this adsorbent. The typical chromatograms of a juice sample after being spiked with OPPs at 100 ng mL⁻¹ are shown in Fig. 7.

Conclusion

In the present work, a new, simple, and one-step method was proposed to prepare a selective and non-toxic sorbent based on immobilization of ZNPs and MNPs in CS as a green and environmental-friendly biopolymer. The fabricated nano-sized sorbent (ZMNIC) presented selective adsorption and extraction of OPPs because of the existence of the ZNPs. Furthermore, ZMNIC was resistant to ZNP leakage in the solution stirring and sonication steps due to suitable immobilization in CS. With the aid of ZMNIC as a super paramagnetic adsorbent, the extraction procedure (isolation of the adsorbent from sample solution and desorption solvent) carried out without limitation because of its relatively high saturation magnetization values. Selective extraction, ease of separation from solution without leakage in the environment, and having high specific area due to its ZNP/MNP content with super paramagnetic property and nano-sized dimensions are three essential features of the synthesized sorbent. Therefore, satisfactory relative recoveries from real samples were obtained, indicating the potential of the synthesized sorbent for selective, accurate, and sensitive detection of OPPs in complicated matrices. Some analytical features of the current method and other recent methods for the extraction and determination of OPPs are compared in Table 4. As shown, the proposed method possesses a wide dynamic range, low LODs, short extraction time, and satisfactory recoveries compared with most of the other reported methods, which could be related to the great adsorptive ability of ZMNIC toward OPPs. The results revealed that the synthesized sorbent can be applied in a simple, fast, and effective MDMSPE procedure for OPP extraction

from various matrices. In addition, the proposed procedure which is reported for the first time can be applied to the synthesis of other magnetic sorbents like ZMNIC with various modifying compounds providing an excellent perspective in the fabrication of selective solid phases without the need for separation methods (filtration and centrifugation).

Compliance with Ethical Standards

Funding The financial support of this work was provided by the Research Council of Ahvaz Jundishapur University of Medical Sciences and Nanotechnology Research Center under grant number GP 94108. This paper is an extract from Miss Behrouz's thesis.

Conflict of Interest Nadereh Rahbar declares that she has no conflict of interest. Elnaz Behrouz declares that she has no conflict of interest. Zahra Ramezani declares that she has no conflict of interest.

Ethical Approval This article does not contain any studies with human participants or animals performed by any of the authors.

Informed Consent Not applicable.

References

- Asgharinezhad AA, Mollazadeh N, Ebrahimzadeh H, Mirbabaei F, Shekari N (2014) Magnetic nanoparticle-based dispersive micro-solid-phase extraction as a novel technique for coextraction of acidic and basic drugs from biological fluids and wastewater. *J Chromatogr A* 1338:1–8
- Bagheri H, Khanipour P, Asgari S (2016a) Magnetic field assisted μ -solid phase extraction of anti-inflammatory and loop diuretic drugs by modified polybutylene terephthalate nanofibers. *Anal Chim Acta* 934:88–97
- Bagheri H, Rezvani O, Banihashemi S (2016b) Core-shell electrospun polybutylene terephthalate/polypyrrole hollow nanofibers for micro-solid phase extraction. *J Chromatogr A* 1434:19–28
- Chaufer B, Rabiller-Baudry M, Bouguen A, Labbe JP, Quémerais A (2000) Spectroscopic characterization of zirconia coated by polymers with amine groups. *Langmuir* 16:1852–1860

- Farajzadeh MA, Afshar Mogaddam MR, Rezaee Aghdam S, Nouri N, Bamorrowat M (2016) Application of elevated temperature–dispersive liquid–liquid microextraction for determination of organophosphorus pesticides residues in aqueous samples followed by gas chromatography–flame ionization detection. *Food Chem* 212:198–204
- Galán-Cano F, Lucena R, Cárdenas S, Valcárcel M (2013) Dispersive micro-solid phase extraction with ionic liquid-modified silica for the determination of organophosphate pesticides in water by ultra performance liquid chromatography. *Microchem J* 106:311–317
- Gong J, Miao X, Wan H, Song D (2012) Facile synthesis of zirconia nanoparticles-decorated graphene hybrid nanosheets for an enzymeless methyl parathion sensor. *Sens Actuat B* 162:341–347
- Guart A, Calabuig I, Lacorte S, Borrell A (2014) Continental bottled water assessment by stir bar sorptive extraction followed by gas chromatography-tandem mass spectrometry (SBSE-GC-MS/MS). *Environ Sci Poll Res* 21:2846–2855
- Heidari H, Razmi H (2012) Multi response optimization of magnetic solid phase extraction based on carbon coated Fe₃O₄ nanoparticles using desirability function approach for the determination of the organophosphorus pesticides in aquatic samples by HPLC–UV. *Talanta* 99:13–21
- Jana S, Trivedi MK, Tallapragada RM, Branton A, Trivedi D, Nayak G, Mishra RK (2015) Characterization of physicochemical and thermal properties of chitosan and sodium alginate after biofield treatment. *Pharmaceu Anal Acta* 6:1000430
- Jiang H, Chen P, Luo S, Tu X, Cao Q, Shu M (2013) Synthesis of novel nanocomposite Fe₃O₄/ZrO₂/chitosan and its application for removal of nitrate and phosphate. *Appl Surf Sci* 284:942–949
- Jiang L, Huang T, Feng S, Wang J (2016) Zirconium(IV) functionalized magnetic nanocomposites for extraction of organophosphorus pesticides from environmental water sample. *J Chromatogr A* 1456:49–57
- Khayoon WS, Saad B, Salleh B, Manaf NHA, Latiff AA (2014) Micro-solid phase extraction with liquid chromatography–tandem mass spectrometry for the determination of aflatoxins in coffee and malt beverage. *Food Chem* 147:287–294
- Korba K, Pelit L, Pelit FO, Özdokur KV, Ertaş H, Eroğlu AE, Ertaş FN (2013) Preparation and characterization of sodium dodecyl sulfate doped polypyrrole solid phase micro extraction fiber and its application to endocrine disruptor pesticide analysis. *J Chromatogr B* 929:90–96
- Kwon OH, Kim JO, Cho DW, Kumar R, Baek SH, Kurade MB, Jeon BH (2016) Adsorption of As(III), As(V) and Cu(II) on zirconium oxide immobilized alginate beads in aqueous phase. *Chemosphere* 160:1:26–133
- Li C, Chen L, Li W (2013) Magnetic titanium oxide nanoparticles for hemimicelle extraction and HPLC determination of organophosphorus pesticides in environmental water. *Microchim Acta* 180:1109–1116
- Li JW, Wang YL, Yan S, Li XJ, Pan SY (2016) Molecularly imprinted calixarene fiber for solid-phase microextraction of four organophosphorus pesticides in fruits. *Food Chem* 192:260–267
- Lin YF, Chen JH, Hsu SH, Hsiao HC, Chung TW, Tung KL (2012) The synthesis of Lewis acid ZrO₂ nanoparticles and their applications in phospholipid adsorption from *Jatropha* oil used for biofuel. *J Colloid Interf Sci* 368:660–662
- Liu H, Sun X, Yin C, Hu C (2008) Removal of phosphate by mesoporous ZrO₂. *J Hazard Mater* 151:616–622
- Liu X, Zhang H, Ma Y, Wu X, Meng L, Guo Y, Yu G, Liu Y (2013) Graphene-coated silica as a highly efficient sorbent for residual organophosphorus pesticides in water. *J Mater Chem A* 1:1875–1884
- Lozano A, Rajska L, Uclés S, Belmonte-Valles N, Mezcuca M, Fernández-Alba AR (2014) Evaluation of zirconium dioxide-based sorbents to decrease the matrix effect in avocado and almond multi residue pesticide analysis followed by gas chromatography tandem mass spectrometry. *Talanta* 118:68–83
- Machala L, Zboril R, Gedanken A (2007) Amorphous iron(III) oxides—a review. *J Phys Chem B* 111:4003–4018
- Maddah B, Shamsi J (2012) Extraction and preconcentration of trace amounts of diazinon and fenitrothion from environmental water by magnetite octadecylsilane nanoparticles. *J Chromatogr A* 1256:40–45
- Mahpishanian S, Sereshti H (2016) Three-dimensional graphene aerogel-supported iron oxide nanoparticles as an efficient adsorbent for magnetic solid phase extraction of organophosphorus pesticide residues in fruit juices followed by gas chromatographic determination. *J Chromatogr A* 1443:43–53
- Mahpishanian S, Sereshti H, Baghdadi M (2015) Superparamagnetic core–shells anchored onto graphene oxide grafted with phenylethyl amine as a nano-adsorbent for extraction and enrichment of organophosphorus pesticides from fruit, vegetable and water samples. *J Chromatogr A* 1406:48–58
- Mazloum-Ardakani M, Beitollahi H, Amini MK, Mirkhalaf F, Abdollahi-Alibeik M (2010) New strategy for simultaneous and selective voltammetric determination of norepinephrine, acetaminophen and folic acid using ZrO₂ nanoparticles-modified carbon paste electrode. *Sens Actuat B* 151:243–249
- Naing NN, Li SFY, Lee HK (2016) Magnetic micro-solid-phase-extraction of polycyclic aromatic hydrocarbons in water. *J Chromatogr A* 1440:23–30
- Namdeo M, Bajpai SK (2008) Chitosan–magnetite nanocomposites (CMNs) as magnetic carrier particles for removal of Fe(III) from aqueous solutions. *Collo Surf A: Physicochem Engin Aspec* 320:161–168
- Parham H, Pourreza N, Rahbar N (2009) Solid phase extraction of lead and cadmium using solid sulfur as a new metal extractor prior to determination by flame atomic absorption spectrometry. *J Hazard Mater* 163:588–592
- Parham H, Rahbar N (2009) Solid phase extraction–spectrophotometric determination of fluoride in water samples using magnetic iron oxide nanoparticles. *Talanta* 80:664–669
- Parham H, Rahbar N (2010) Square wave voltammetric determination of methyl parathion using ZrO₂-nanoparticles modified carbon paste electrode. *J Hazard Mater* 177:1077–1084
- Parham H, Zargar B, Shiralipour R (2012) Fast and efficient removal of mercury from water samples using magnetic iron oxide nanoparticles modified with 2-mercaptobenzothiazole. *J Hazard Mater* 205:206:94–100
- Peng Q, Liu Y, Zeng G, Xu W, Yang C, Zhang J (2010) Biosorption of copper(II) by immobilizing *Saccharomyces cerevisiae* on the surface of chitosan-coated magnetic nanoparticles from aqueous solution. *J Hazard Mater* 177:676–682
- Peng XT, Jiang L, Gong Y, XZ H, Peng LJ, Feng YQ (2015) Preparation of mesoporous ZrO₂-coated magnetic microsphere and its application in the multi-residue analysis of pesticides and PCBs in fish by GC–MS/MS. *Talanta* 132:118–125
- Plotka-Wasyłka J, Szczepańska N, de la Guardia M, Namieśnik J (2015) Miniaturized solid-phase extraction techniques. *TrAC Trend Anal Chem* 73:19–38
- Sang ZY, Wang YT, Tsoi YK, Leung KS (2013) CODEX-compliant eleven organophosphorus pesticides screening in multiple commodities using headspace-solid phase microextraction-gas chromatography-mass spectrometry. *Food Chem* 136:710–717
- Shi ZG, Feng YQ, Xu L, Zhang M, Da SL (2004) Preparation and evaluation of zirconia-coated silica monolith for capillary electrochromatography. *Talanta* 63:593–598
- Sohn JR, Kwon TD, Kim SB (2001) Characterization of zirconium sulfate supported on zirconia and activity for acid catalysis. *Bull Kor Chem Soc* 22:1309–1315
- Volante M, Galarini R, Miano V, Cattaneo M, Pecorelli I, Bianchi M, Marinoni MT, Cossingnani L, Damiani P (2001) A SPME-GC-MS approach for Antivarroa and pesticide residues analysis in honey. *Chromatographia* 54:241–246
- Wang J, Chen Z, Li Z, Yang Y (2016) Magnetic nanoparticles based dispersive micro-solid-phase extraction as a novel technique for

- the determination of estrogens in pork samples. *Food Chem* 204: 135–140
- Wang M, Li Z (2008) Nano-composite ZrO_2/Au film electrode for voltammetric detection of parathion. *Sens Actuat B* 133:607–612
- Wang YL, Gao YL, Wang PP, Shang H, Pan SY, Li XJ (2013) Sol-gel molecularly imprinted polymer for selective solid phase microextraction of organophosphorous pesticides. *Talanta* 115: 920–927
- Wu J, Zhao H, Xiao D, Chuong PH, He J, He H (2016) Mixed hemimicelles solid-phase extraction of cephalosporins in biological samples with ionic liquid-coated magnetic graphene oxide nanoparticles coupled with high-performance liquid chromatographic analysis. *J Chromatogr A* 1454:1–8
- Xie J, Liu T, Song G, Hu Y, Deng C (2013) Simultaneous analysis of organophosphorus pesticides in water by magnetic solid-phase extraction coupled with GC–MS. *Chromatographia* 76:535–540
- Yilmaz E, Soylak M (2016) Preparation and characterization of magnetic carboxylated nanodiamonds for vortex-assisted magnetic solid-phase extraction of ziram in food and water samples. *Talanta* 158: 152–158
- Zare M, Ramezani Z, Rahbar N (2016) Development of zirconia nanoparticles-decorated calcium alginate hydrogel fibers for extraction of organophosphorous pesticides from water and juice samples: facile synthesis and application with elimination of matrix effects. *J Chromatogr A* 1473:28–37
- Zhou L, Liu Z, Liu J, Huang Q (2010) Adsorption of Hg(II) from aqueous solution by ethylenediamine-modified magnetic crosslinking chitosan microspheres. *Desalination* 258:41–47
- Zong E, Wei D, Wan H, Zheng S, Xu Z, Zhu D (2013) Adsorptive removal of phosphate ions from aqueous solution using zirconia-functionalized graphite oxide. *Chem Engin J* 221:193–203